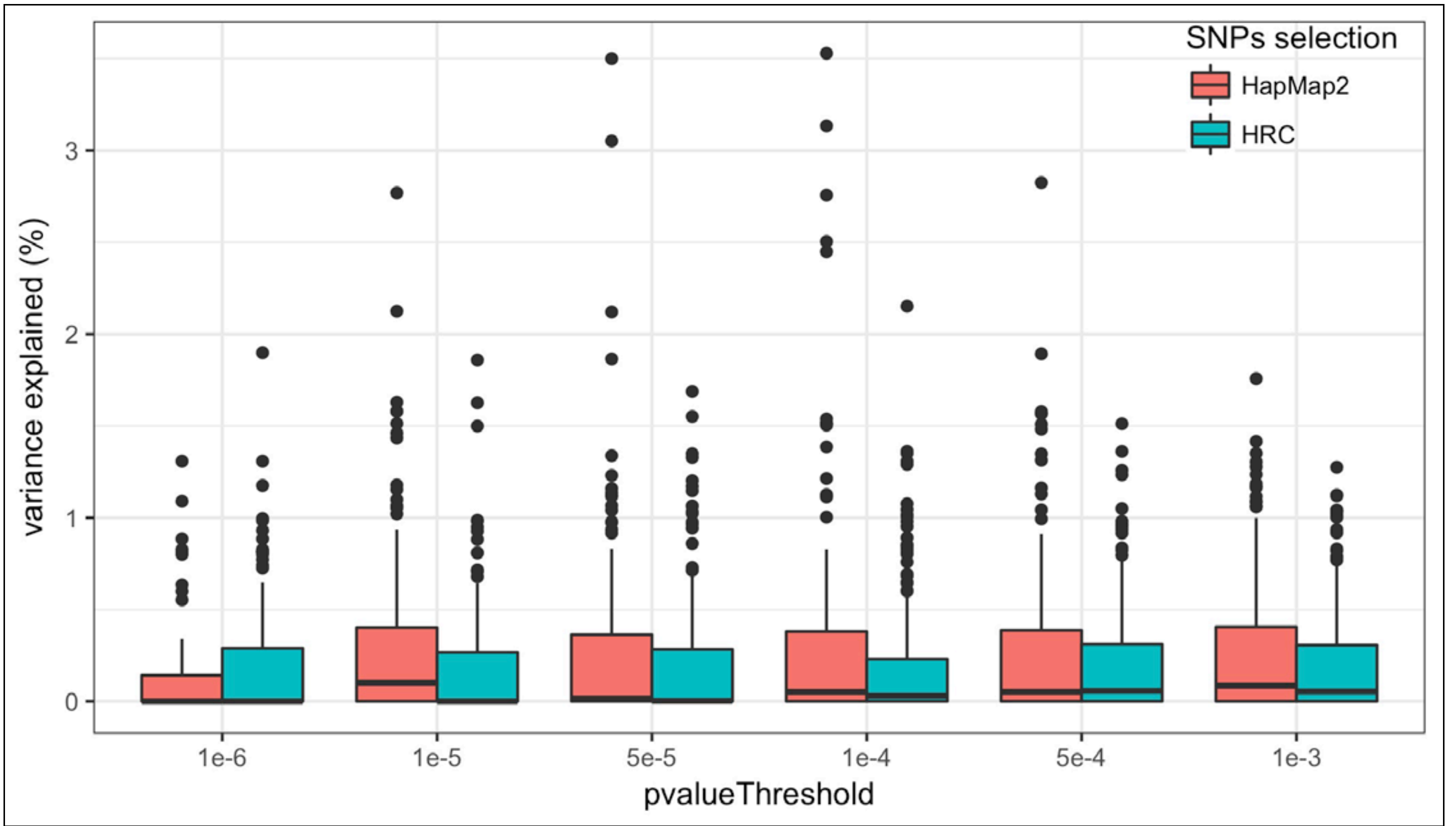

Supplementary Figure 1

Distribution of variance explained for microbiome features in 500FG.

Distribution of variance explained of microbiome features in 445 normo-glycemic 500FG individuals by genetic predictors selected in LL-DEEP GWAS at different P-value thresholds, when predictors are selected from the full HRC imputed data (green), or when restricted to HapMap2 SNPs and proxies (red). Distributions are represented as boxplots, where the box hinges represent the 25th and 75th percentile, the central line of the box represents the median value, and the points outliers (default options in the *boxplot*() function in R).

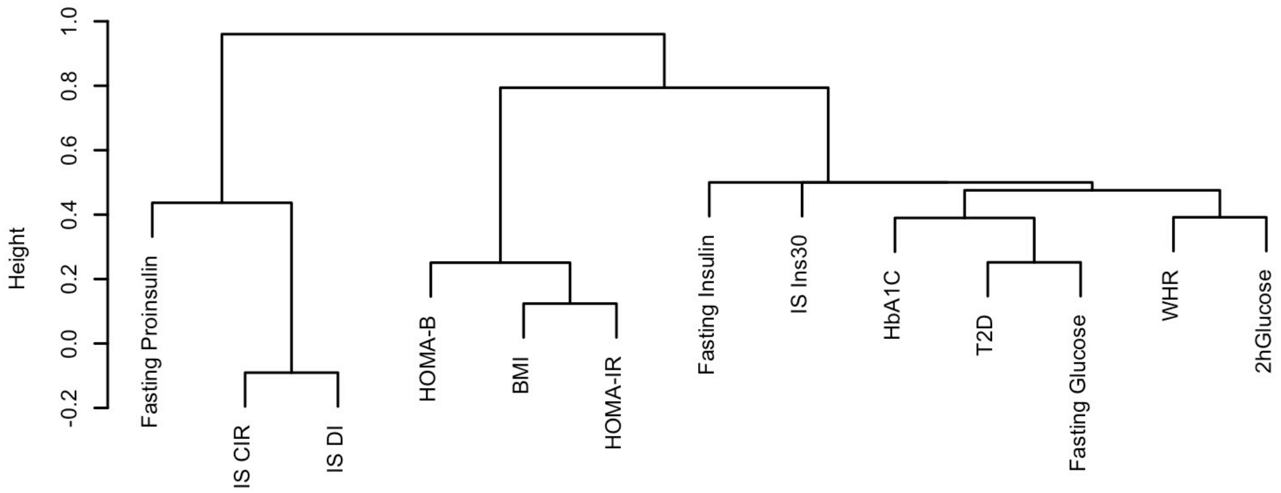

Supplementary Figure 2
Clustering of metabolic traits using genetic correlation.
Clustering of metabolic traits generated using the R function *hclust*(“complete”) and a dissimilarity metric of $(1-\rho_g)/2$, where ρ_g is the genetic correlation.

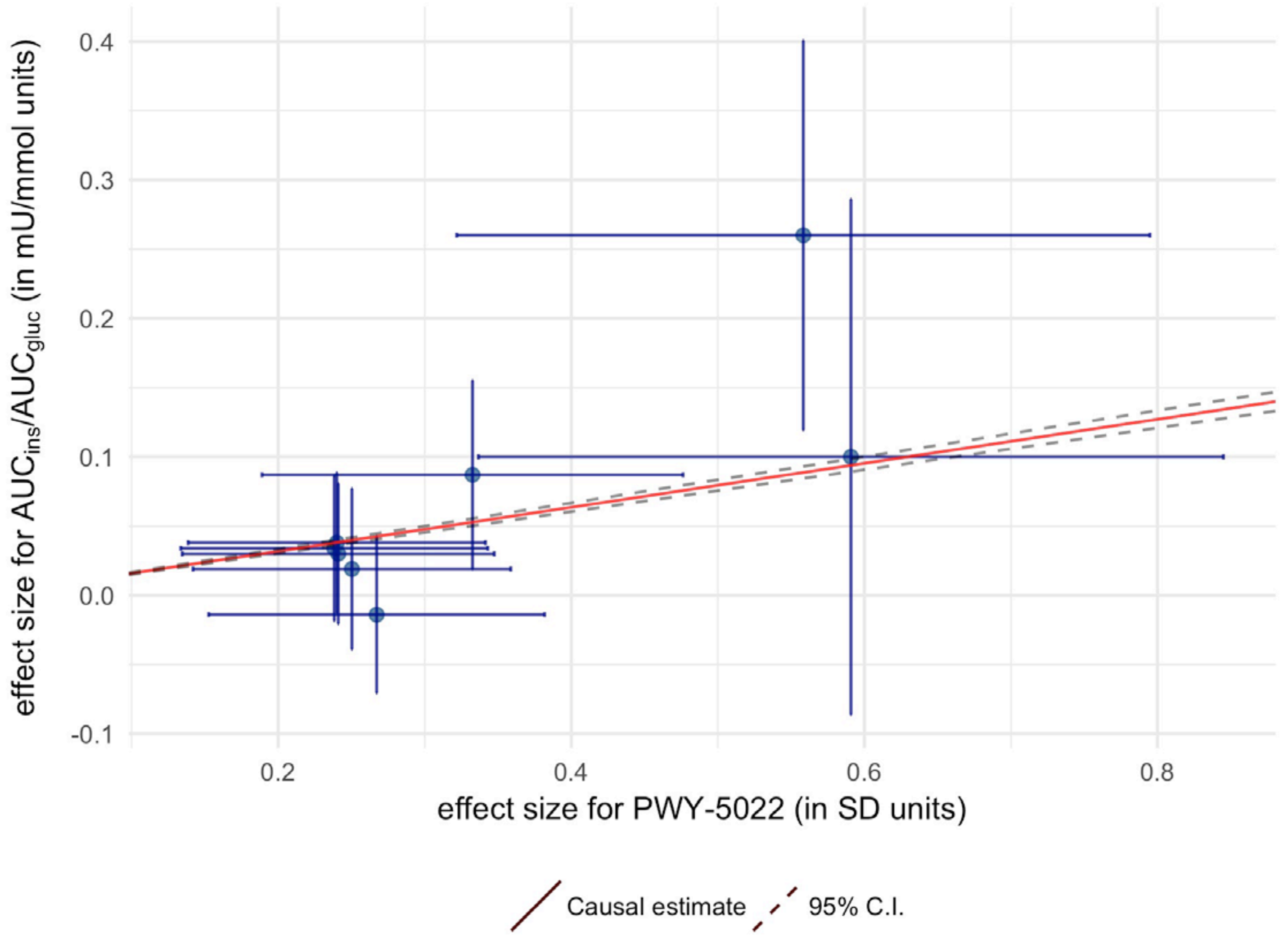

Supplementary Figure 3

Mendelian Randomization plot showing the causal effect of microbiome PWY-5022 on glucose-stimulated insulin response.

In this plot, each point is a genetic predictor of PWY-5022. The x-axis plot shows their effect size on PWY-5022 as estimated in LL-DEEP cohort (952 samples), and the y-axis shows the allelic effect on glucose-stimulated insulin response as estimated in MAGIC (4213 samples). Whiskers represent 95% confidence intervals of these effects. The slope of the red line represents the causal effect estimated by the Mendelian Randomization analysis with the IVW test, with dashed lines corresponding to 95% confidence interval (as given in **Supplementary Table 5**)

MR estimate Test	MR estimate p	Pleiotropy Test	Pleiotropy p
IVW	9.8e-05		
MR-PRESSO	0.02	MR-PRESSO Global test	0.18
Weighted Median	0.02		
MR-EGGER	0.02	Rucker Q' (modified)	0.77

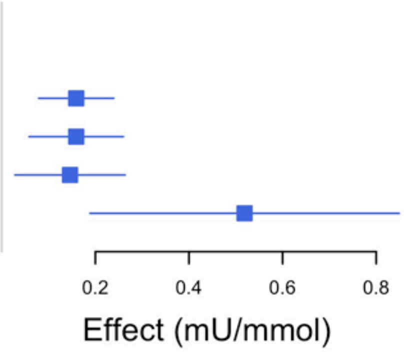

Supplementary Figure 4

Forest plot of the PWY-5022 causal effect estimated with different statistical tests.

The forest plot shows the causal effect (in mU/mmol) of PWY-5022 on glucose-stimulated insulin response parameter $AUC_{insulin}/AUC_{glucose}$ estimated with different MR tests, using 8 genetic predictors and their effects from LL-DEEP (952 samples) and MAGIC (4213 samples) summary statistics. Bars represent 95% confidence intervals. The annexed table indicates the two-sided pvalues for the respective MR and pleiotropy statistical tests.

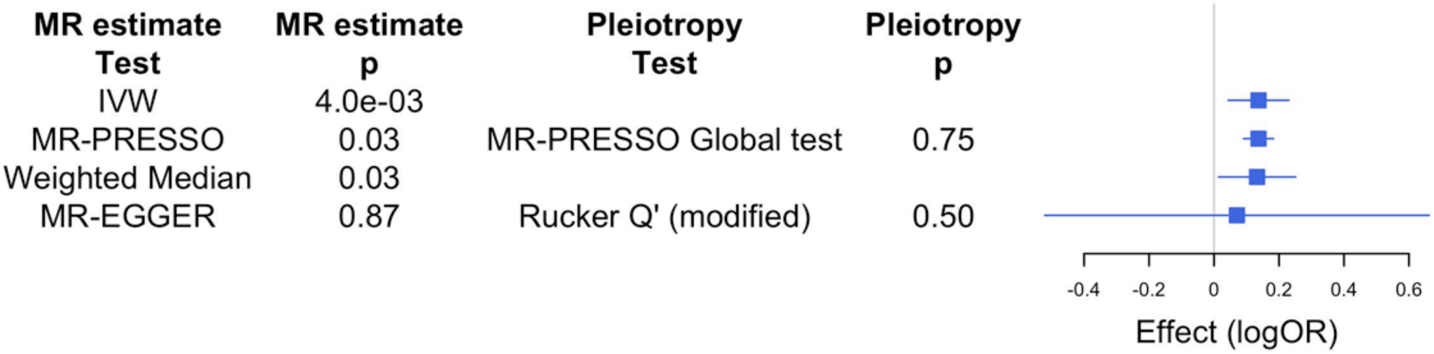

MR estimate Test	MR estimate p	Pleiotropy Test	Pleiotropy p
IVW	4.0e-03		
MR-PRESSO	0.03	MR-PRESSO Global test	0.75
Weighted Median	0.03		
MR-EGGER	0.87	Rucker Q' (modified)	0.50

Supplementary Figure 5

Forest plot of the fecal propionate causal effect on T2D estimated with different statistical tests.

The forest plot shows the causal effect (in log(OR) units) of fecal propionate on T2D estimated with different MR tests, using 3 genetic predictors and their effects from LL-DEEP (898 samples) and DIAGRAM (26,676 T2D cases and 132,532 controls) summary statistics. Bars represent 95% confidence intervals. The annexed table indicates the two-sided pvalues for the respective MR and pleiotropy statistical tests.

MR estimate Test	MR estimate p	Pleiotropy Test	Pleiotropy p
IVW	6.8e-03		
MR-PRESSO	0.07	MR-PRESSO Global test	2.0e-03
Weighted Median	0.76		
MR-EGGER	0.92	Rucker Q' (modified)	9.2e-04

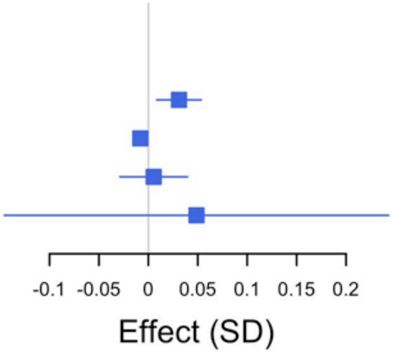

Supplementary Figure 6

Forest plot of the fecal propionate causal effect on BMI estimated with different statistical tests.

The forest plot shows the causal effect of fecal propionate on BMI (in SD units) estimated with different MR tests using 3 genetic predictors and their effects from LL-DEEP (898 samples) and GIANT (339,224 samples) summary statistics. Bars represent 95% confidence intervals. The annexed table indicates the two-sided pvalues for the respective MR and pleiotropy statistical tests.